HHS Public Access

Author manuscript

Mol Cancer Ther. Author manuscript; available in PMC 2019 October 01.

Published in final edited form as:

Mol Cancer Ther. 2018 October ; 17(10): 2079–2090. doi:10.1158/1535-7163.MCT-18-0117.

Therapeutic Potential of Leelamine, a Novel Inhibitor of Androgen Receptor and Castration-Resistant Prostate Cancer

Krishna B. Singh[1], **Xinhua Ji**[2], and **Shivendra V. Singh**[1,3]

[1]Department of Pharmacology & Chemical Biology, University of Pittsburgh School of Medicine, Pittsburgh, Pennsylvania. [2]Macromolecular Crystallography Laboratory, National Cancer Institute, Frederick, Maryland. [3]UPMC Hillman Cancer Center, University of Pittsburgh School of Medicine, Pittsburgh, Pennsylvania.

Abstract

Clinical management of castration-resistant prostate cancer (CRPC) resulting from androgen deprivation therapy remains challenging. CRPC is driven by aberrant activation of androgen receptor (AR) through mechanisms ranging from its amplification, mutation, post-translational modification, and expression of splice variants (e.g., AR-V7). Herein, we present experimental evidence for therapeutic vulnerability of CRPC to a novel phytochemical, leelamine (LLM), derived from pine tree bark. Exposure of human prostate cancer cell lines LNCaP (an androgen-responsive cell line with mutant AR), C4–2B (an androgen-insensitive variant of LNCaP), and 22Rv1 (a CRPC cell line with expression of AR-Vs), and a murine prostate cancer cell line Myc-CaP to plasma achievable concentrations of LLM resulted in ligand-dependent (LNCaP) and ligand-independent (22Rv1) growth inhibition *in vitro* that was accompanied by downregulation of mRNA and/or protein levels of full-length AR as well as its splice variants including AR-V7. LLM treatment resulted in apoptosis induction in the absence and presence of R1881. *In silico* modelling followed by luciferase reporter assay revealed a critical role for non-covalent interaction of LLM with Y739 in AR activity inhibition. Substitution of the amine group with an isothiocyanate functional moiety abolished AR and cell viability inhibition by LLM. Administration of LLM resulted in 22Rv1 xenograft growth suppression that was statistically insignificant but was associated with a significant decrease in Ki-67 expression, mitotic activity, expression of full-length AR and AR-V7 proteins, and secretion of prostate-specific antigen. The present study identifies a novel chemical scaffold for the treatment of CRPC.

Keywords

Androgen Receptor; Castration-Resistant Prostate Cancer; Leelamine; Prostate Cancer

Corresponding Author: Shivendra V. Singh, 2.32A UPMC Hillman Cancer Center Research Pavilion, 5117 Centre Avenue, Pittsburgh, PA 15213. Phone: 412-623-3263; Fax: 412-623-7828; E-mail: singhs@upmc.edu.

Conflict of interest: The authors do not have any conflict of interest.

Introduction

Prostate cancer continues to be a leading cause of cancer-related deaths among men in western countries despite rigorous screening efforts for early detection of the disease (1). The American Cancer Society estimates diagnosis of about 165,000 new cases of prostate cancer and over 29,000 deaths from this malignancy in the United States alone in 2018. Androgen-receptor (AR) plays an important role in prostate cancer pathogenesis (2–4). AR signalling axis, which is essential for normal male reproductive function, is activated after binding of androgens (e.g., dihydrotestosterone) to the receptor, leading to its nuclear trafficking for subsequent regulation of transcriptional targets, including prostate-specific antigen (PSA) and transmembrane protease, serine 2 (TMPRSS2) (2–4). Androgen deprivation therapy (ADT) is the standard of care for initial systemic treatment of localized and advanced prostate cancer (5, 6). Unfortunately, a great majority of patients on ADT eventually progresses to castration-resistant prostate cancer (CRPC) within 2–3 years (5, 6). Clinically available therapeutic options for advanced and metastatic prostate cancer include anti-androgens such as abiraterone acetate (an irreversible inhibitor of CYP17A1) or enzalutamide, a nonsteroidal antiandrogen (7, 8). However, a subset of patients is inherently resistant to both abiraterone (Zytiga) and enzalutamide (Xtandi) due to expression of constitutively active splice variants of AR like AR-V7 (9). Therefore, identification of novel agents effective against CRPC expressing splice variants of AR is still desirable.

The molecular understanding of the changeover from androgen dependence to CRPC continues to evolve but AR occupies a central place in this transition (10–13). AR is a 110 kDa transcription factor belonging to the steroid hormone receptor superfamily (2–4). Full-length AR comprises of four major functional domains including an N-terminal domain, a DNA-binding domain, a hinge region containing the nuclear localization sequence, and the C-terminal ligand-binding domain (4). Continued dependence on the AR is partly accountable for CRPC development, which may be driven by mechanisms ranging from increased amplification or gain-of-function mutations to ligand-independent activation and expression of C-terminally truncated and constitutively active splice variants (14–18).

The search for novel small molecule inhibitors of AR continues because of the mechanistic complexity of its aberrant activation in CRPC. Naturally-occurring phytochemicals abundant in edible or medicinal plants remain attractive for treatment of cancer (19, 20). The present study identifies a novel chemical scaffold, leelamine (LLM, also known as dehydroabietylamine), with activity in human prostate cancer cells. LLM is derived from the bark of pine tree. Growth inhibitory effects of LLM have been studied previously in melanoma cell lines *in vitro* and *in vivo* (21, 22). However, the present study is the first to demonstrate inhibition of AR expression and activity in prostate cancer cells (LNCaP, C4–2B, 22Rv1, and Myc-CaP), including a cell line that is resistant to enzalutamide (22Rv1). We also provide *in vivo* evidence for LLM-mediated inhibition of AR expression and its downstream targets (PSA) using 22Rv1 xenograft model. A functionally important non-covalent interaction between LLM and ligand binding domain of AR is also shown.

Materials and Methods

Ethics statement

Use of mice for this study was approved by the University of Pittsburgh Animal Care and Use Committee.

Reagents

LLM (purity ≥ 98%) was purchased from Cayman Chemical Company (Ann Arbor, MI). Dehydroabietyl isothiocyanate (LLM-ITC) was purchased from American Custom Chemicals Corp (San Diego, CA), whereas enzalutamide was purchased from Sigma-Aldrich (St. Louis, MO). Reagent for cell culture were purchased from Life technologies-Thermo Fisher Scientific (Waltham, MA), and charcoal-dextran-stripped fetal bovine serum (cFBS) was purchased from Hyclone (GE Healthcare; Logan, UT). The synthetic androgen R1881 was purchased from Perkin- Elmer (Boston, MA). The antibody against AR was purchased from Santa Cruz Biotechnology (Dallas, TX). The anti-prostate-specific antigen (PSA; A0562) antibody was from Dako-Agilent Technologies (Carpinteria, CA). An antibody against phospho-AR (Ser210/213) was purchased from Imgenex-Novus Biologicals (Littleton, CO). FuGENE 6, Dual-Luciferase Reporter Assay kit, and pRL-CMV were purchased from Promega (Madison, WI). AR mutant plasmid pCMV-AR-Y739A was kindly provided by Dr. Elizabeth M. Wilson (University of North Carolina, Chapel Hill, USA). The rat probasin promoter plasmid p159pPr-luc was a gift from Jeffery Green (Addgene plasmid #8392).

Cell lines and culture conditions

The 22Rv1 and LNCaP cells were obtained from the American Type Culture Collection (Manassas, VA). These cell lines were last authenticated by us in March of 2017 and found to be of human origin. The C4–2B cell line was obtained from UroCor (Oklahoma City, OK), and last authenticated by us in January of 2015. The 22Rv1, LNCaP, and C4–2B cells were maintained in RPMI1640 supplemented with 10% FBS, antibiotic mixture, sodium pyruvate, HEPES, and 2.5 g/L glucose. Myc-CaP cells were kindly provided by Dr. Charles L. Sawyers (Department of Medicine, University of California, CA). This cell line was not authenticated by us. The Myc-CaP cells were maintained in Dulbecco's Modified Eagles Medium supplemented with 10% FBS, and antibiotic mixture. Normal human prostate cells (PrSC) were purchased from Lonza (Walkersville, MD), and cultured in growth medium supplied by the provider. The PC3 cells with stable overexpression of GFP-AR (PC3-AR) were a generous gift by Dr. Zhou Wang (Department of Urology, University of Pittsburgh, PA). The PC3-AR cells were not authenticated by us. PC3-AR and corresponding empty vector transfected cells (PC3-EV) were maintained in RPMI1640 medium supplemented with 10% fetal bovine serum and G418 (600 μg/mL). For the experiments that required androgen depleted condition, cells were maintained in phenol red-free media supplemented with 10% cFBS.

Cell viability assay

The effects of LLM, enzalutamide, and LLM-ITC on cell viability were determined by trypan blue dye exclusion assay as described by us previously (23). Briefly, prostate cancer cells or PrSC cells were seeded in 12-well plates, and allowed to attach by overnight incubation. The cells were then treated with the specified concentrations of the test agents for 24 or 48 hours. Cells were trypsinized and stained with trypan blue. The live cells were counted under an inverted microscope.

Cell proliferation assay

LNCaP cells or C4–2B cells (750 cells/well) were seeded in 96-well plates. After 16 hours of incubation, cells were treated with ethanol (control) or the indicated doses of LLM or synthetic androgen R1881 for 24, 48, and 72 hours. Subsequently, 20 μL of manufacturer supplied colour development reagent (MTS, Promega, Madison, WI) was added to each well and the plates were incubated at 37°C for 2 hours. Absorbance was measured at 492 nm.

Clonogenic assay

Cells (500 cells per well) were seeded in 6-well plates. After overnight incubation to allow attachment of the cells, they were treated with different concentrations of LLM. The medium containing ethanol (control) or LLM was replaced every third day. After 10 days of treatment, cells were rinsed with phosphate-buffered saline (PBS), fixed with 100% methanol for 5 minutes, and stained with 0.5% crystal violet solution in 20% methanol for 30 minutes at room temperature. The colonies were counted using GelCount (Oxford Optronix, Abingdon, UK).

Western blotting

Details of lysate preparation and immunoblotting have been described by us previously (24). The cells were treated with desired concentrations of LLM or its analog for different time points. Western blot analysis was performed as described previously by us (24). In some experiments, cells were pretreated with 1.5 μmol/L of MG132 for 1 hour followed by treatment with LLM for an additional 12 hours.

Microscopy for nuclear translocation of AR

The 22Rv1 (7×10^4) or LNCaP (5×10^4) cells were plated in triplicate on coverslips in 12-well plates in phenol red-free medium supplemented with 10% cFBS and allowed to attach by overnight incubation. Cells were treated with ethanol or LLM for 3 hours followed by addition of R1881. The plates were incubated for an additional 9 hours. The cells were washed with PBS and fixed in 2% paraformaldehyde for 1 hour followed by blocking with a solution containing 0.5% bovine serum albumin and 0.15% glycine in PBS. After blocking, cells were incubated with AR antibody (4°C; overnight) followed by treatment with Alexa Fluor 488-conjugated secondary antibody for 1 hour at room temperature. The cells were counterstained with 4’,6-diamidino-2-phenylindole (DAPI; 50 ng/mL) and examined under a Leica DC 300F fluorescence microscope.

RNA isolation and real-time reverse transcription polymerase chain reaction (RT-PCR)

The expression of *AR* mRNA and its target genes (*PSA* and *TMPRSS2*) were determined by RT-PCR. Total RNA from ethanol- and LLM-treated cells was isolated using RNeasy kit. One μg RNA was used for cDNA synthesis with the use of SuperScript III reverse transcriptase and oligo $(dT)_{20}$ primer. Quantitative PCR was performed using 2× SYBR Green master mix for 40 cycles. The expression of *AR* and its target genes were normalized to glyceraldehyde 3-phosphate dehydrogenase (*GAPDH*). The primers for human *AR, PSA, TPMRSS2*, and *GAPDH* were as follows: Forward (*AR*): 5'-ATGGTGAGCAGAGTGCCCTA-3'; reverse (*AR*) 5'-GTGGTGCTGGAAGCCTCTCCT-3'; forward (*PSA*): 5'-AAAAGCGTGATCTTGCTGGG-3'; reverse (*PSA*): 5'-CATGACCTTCACAGCATCCG-3'; forward (*TMPRSS2*): TCTAACTGGTGTGATGGCGT-3'; reverse (*TMPRSS2*): 5'-GGATCCGCTGTCATCCACTA-3'; 5'- forward (*GAPDH*): 5'-GGACCTGACCTGCCGTCTAGAA-3'; reverse (*GAPDH*): 5'-GGTGTCGCTGTTGAAGTCAGAG-3'. The PCR conditions were as follows: 95°C for 10 minutes followed by 40 cycles of 95°C for 15 seconds, 60°C (*AR, TMPRSS2, and GAPDH*) and 63°C (*PSA*) for 1 minute, and 72°C for 30 seconds.

Quantitation of PSA in cell culture medium

Desired cells (22Rv1 and LNCaP- $5–7\times10^4$) were plated in triplicate in 12-well plates in phenol red-free medium containing 10% cFBS. After attachment, cells were treated with ethanol or LLM for 24 hours. Media were collected and centrifuged at 3500 rpm for 15 minutes. Equal volume of supernatant was used to determine PSA levels using Quantikine Human KLK3/PSA Immunoassay kit from R&D Systems (Minneapolis, MN).

Apoptosis assay

The 22Rv1 or LNCaP cells were plated in triplicate in phenol red-free media containing cFBS and allowed to attach by overnight incubation. The cells were then treated with ethanol, 1 nmol/L R1881 and/or indicated doses of LLM for 24 hours. Apoptosis was quantified by analysis of histone-associated DNA fragment release into the cytosol or by flow cytometry after staining the cells with Annexin V/propidium iodide as described by us previously (25).

Molecular docking

Molecular docking for the ligand binding domain (LBD) of AR with LLM or LLM-ITC was performed using HEX 8.0 software. The coordinates for LLM and LLM-ITC were taken from the SDF files and converted into pdb format using Discovery Studio 4.1 software. The crystal structure of AR (PDB ID: 2PIW) was retrieved from the Protein Data Bank (http://www.rcsb.org./pdb). Visualization of the model was performed using Discovery Studio 4.0 software. A "by default" parameter was used for the docking calculation with correlation type shape only, FFT mode at 3D level, grid dimension of 6 with receptor range 180 and ligand range 180 with twist range 360 and distance range 40. The resulting models were visually inspected, during which one minor adjustment was made to eliminate a steric conflict between LLM and an amino acid side chain on the surface of AR LBD.

Transient transfection and luciferase reporter assay

PC-3 cells (4×10^4) were plated in triplicate in phenol red-free Opti-MEM medium containing 10% cFBS and 10 nM R1881. The cells were co-transfected with 2 μg of mutant AR or 2 μg of rat probasin luciferase (pPr-luc) and 0.5 μg pCMV-RL plasmid for 24 hours. After transfection, cells were treated with ethanol or LLM for 12 hours. The transient transfection was achieved using FuGENE6. Luciferase activity was measured using Dual-Luciferase Reporter Assay System (Promega) following the manufacturer's protocol.

Xenograft study

Twelve male SCID (NOD.CB17-PRkdc$^{scid/J}$) mice at 4–5 weeks of age were purchased from Jackson Laboratories (Bar Harbor, ME). After a 5-day acclimation, fur was removed from the torso of each animal in the area directly above each hind limb using scissors. Both sides of each mouse in that area were injected with 2×10^6 22Rv1 cells suspended in 200 μL of serum-free medium diluted 1:1 with Matrigel (BD Biosciences, San Jose, CA). Cells were grown to approximately 60% confluency to ensure that the cells were in active growth phase. One week post-implantation, the mice were divided into two groups. Mice of group 1 were treated with 100 μL vehicle while group 2 mice received 9.1 mg LLM/kg by intraperitoneal injection 5 times/week. The vehicle consisted of 10% ethanol, 10% dimethyl sulfoxide, 30% Kolliphor EL (Sigma-Aldrich, St. Louis, MO), and 50% PBS. At the onset of the study, mice were weighed and this measurement continued on a weekly basis. Tumor volume measurements were taken using Vernier callipers as soon as tumors became measurable and continued 3 times each week until the conclusion of the study. Treatment continued until the tumor burden exceeded 2000 mm^3 at which time the animals were euthanized by CO_2 overdose (supplied *via* compressed gas cylinder) and blood, tumor tissue, and vital organs were harvested. A portion of each tumor and all vital organs were fixed in 10% neutral buffered formalin for H&E or immunohistochemistry. The other portion of each tumor was placed on dry ice and later stored at −80°C. Blood was collected using a heparinized needle then placed on ice and later centrifuged at 3000 RPM for 5 minutes. Plasma was removed and stored at −20°C.

Immunohistochemistry

Immunohistochemistry was performed as described by us previously (26, 27) with some modifications. Briefly, 4–5 μm thick tumor sections were de-paraffinized, hydrated in graded alcohol, and then washed with PBS. Sections were treated with 0.3% H_2O_2 in 100% methanol for 20 minutes at room temperature and then incubated with the blocking buffer for 1 hour. Subsequently, the tumor sections were treated with the anti-Ki-67 antibody overnight in humid chambers at room temperature. After washing, sections were incubated with horseradish peroxidase-conjugated secondary antibody for 1 hour at room temperature. A characteristic brown stain was developed with 3,3'-diaminobenzidine. Stained sections were examined under a Leica DC300F microscope. At least five non-overlapping representative images were captured from each section, and analysed with the Aperio ImageScope v9.1 software (Aperio, Vista, CA) using nuclear algorithm.

Statistical analysis

Statistical analyses were carried out using GraphPad Prism (version 6.07). Statistical significance of difference was determined by the one-way analysis of variance (ANOVA) followed by Dunnett's or Bonferroni's test or unpaired Student's t-test.

Results

LLM treatment inhibited viability of prostate cancer cells *in vitro* in association with downregulation of AR protein

Two-well characterized human prostate cancer cell lines (22Rv1 and LNCaP), an androgen-insensitive variant of LNCaP cells, a murine prostate cancer cell line (Myc-CaP), and a normal prostate cell line (PrSC) were used to determine the growth inhibitory effect of LLM (structure of LLM is shown in Fig. 1A). Pharmacokinetics of LLM has been determined in male ICR mice after a single oral administration at 10 mg/kg body weight (28). Peak plasma concentration (C_{max}) of LLM was about 2.8 μmol/L with a T_{max} (time to reach C_{max}) of 4.7 hours and plasma half-life of 5.7 hours (28). Therefore, LLM concentrations of 0.5, 1, 2.5, and/or 5 μmol/L were used to determine its effect on viability of prostate cancer cells. LLM treatment inhibited viability of 22Rv1 and LNCaP cells in a concentration-dependent manner (Fig. 1B). Viability of Myc-CaP cell line was also inhibited significantly upon LLM treatment (Supplementary Fig. S1A). However, the inhibitory effect of LLM treatment on viability of Myc-CaP cells was relatively less pronounced compared with 22Rv1 or LNCaP (Supplementary Fig. S1A), which may be attributable to very high expression of the Myc oncoprotein. Further work is necessary to test this possibility, but PrSC cells were relatively more resistant to cell viability inhibition by LLM compared to prostate cancer cells (Fig. 1B). For example, viability of 22Rv1 cells was decreased by >90% after 24-hour treatment with 5 μmol/L LLM. The viability of PrSC was not affected at all after 24-hour treatment with 5 μmol/L LLM (Fig. 1B). We also found that the 22Rv1 cell line was completely resistant to cell viability inhibition by enzalutamide concentrations of 2.5 and 5 μmol/L (Fig. 1C). As expected, the LNCaP cell line, but not 22Rv1, was sensitive to growth stimulation by a synthetic androgen (R1881) (Fig. 1D). The R1881-stimulated growth of LNCaP cell line was also suppressed significantly in the presence of LLM (Fig. 1D). Furthermore, LNCaP and C4–2B cells were more or less equally sensitive to cell proliferation inhibition by LLM regardless of R1881 treatment (Supplementary Fig. S2). Clonogenic assay confirmed cell survival inhibition by LLM (Fig. 1E, F). These results indicated anticancer effect of LLM in prostate cancer cells regardless of the androgen responsiveness.

Treatment of 22Rv1, LNCaP, and C4–2B human prostate cancer cells (Fig. 2A) and the Myc-CaP cell line (Supplementary Fig. S1B, C) with LLM resulted in a dose-dependent suppression of protein levels of full-length AR as well as its splice variants, including AR-V7, and phosphorylated AR. LLM-mediated suppression of full-length AR was evident at both 12- and 24-hour time points. Densitometric quantitation of the full-length AR (22Rv1, LNCaP, and C4–2B) and AR-V7 proteins (22Rv1) in LLM-treated cells normalized to corresponding solvent-treated control are shown in Supplementary Figure S3. An antibody specific for AR-V7 was used to determine the effect of LLM on AR-V7 expression in 22Rv1 cells. Similar to the full-length AR, LLM treatment caused a decrease in protein level of

AR-V7 in 22Rv1 cells (LNCaP or C4–2B cells do not express AR-V7). As can be seen in Fig. 2B, the AR protein was predominantly nuclear in 22Rv1 cells. Nuclear level of AR protein was decreased markedly in the presence of LLM irrespective of the R1881 treatment (Fig. 2B). On the other hand, R1881-stimulated nuclear translocation of AR in LNCaP cells (Supplementary Fig. S4). Similar to the 22Rv1 cells, however, nuclear level of AR protein was reduced following LLM exposure with or without R1881 treatment (Supplementary Fig. S4). Downregulation of AR by LLM treatment was accompanied by suppression of AR target genes *PSA* and *TMPRSS2* (Fig. 2C, D). Consistent with these results, protein levels (Fig. 2E) and/or secretion of PSA (Fig. 2F) were decreased markedly upon treatment of 22Rv1, LNCaP, and C4–2B cells with LLM. Densitometric quantitation of PSA levels in LLM-treated 22Rv1, LNCaP, and C4–2B cell lysates normalized for corresponding solvent control are shown in Supplementary Figure S5. Collectively, these results indicated inhibition of AR expression and activity by LLM treatment in both 22Rv1 and LNCaP cells.

Transcriptional suppression of AR by LLM treatment

Expression of *AR* mRNA was also decreased following LLM treatment in both 22Rv1 and LNCaP cells (Fig. 3A). We used a proteasomal inhibitor (MG132) to determine the role of post-transcriptional mechanisms in AR downregulation by LLM treatment. LLM-mediated downregulation of AR protein expression was not reversed in the presence of MG132 in either cell line (Fig. 3B; Supplementary Fig. S6A). These results indicated transcriptional suppression of AR following LLM treatment.

LLM treatment resulted in apoptotic cell death in prostate cancer cells

Treatment of 22Rv1 and LNCaP cells with LLM resulted in increased release of histone associated DNA fragments into the cytosol, a measure of apoptotic cell death, in comparison with vehicle-treated control, which was not affected by the presence of R1881 (Fig. 3C). The 22Rv1 cell line was relatively more sensitive than LNCaP to apoptosis induction by LLM (Fig. 3C), which was consistent with cell viability inhibition data (Fig. 1B). Annexin V methods confirmed apoptosis induction by LLM treatment regardless of R1881 exposure (Fig. 3D, E).

Overexpression of AR resulted in sensitization of PC-3 cells to growth inhibition by LLM

In comparison with 22Rv1 or LNCaP cells (Fig. 2A), AR protein level was decreased to a lesser extent by LLM treatment in PC-3 cells stably transfected with GFP-AR plasmid (Fig. 3F; Supplementary Fig. S6B). This finding, and the observation that LLM decreases GFP-AR level to a lesser extent in PC-3 cells than in other cell lines makes it more likely that LLM acts to suppress the activity of the endogenous AR promoter (vs. the strong promoter driving GFP-AR expression). Interestingly, overexpression of AR resulted in sensitization of PC-3 cells to growth inhibition by LLM especially at the higher concentrations as revealed by trypan blue dye exclusion assay (Fig. 3G). These results were confirmed by clonogenic assay (Fig. 3H, I). These results indicated that AR is a valid therapeutic target of LLM.

Interaction of LLM with amino acid residues in the ligand binding domain (LBD) of AR

AR is a modular protein consisting of an N-terminal domain, a central zinc-finger DNA-binding domain, a hinge region, and a highly-structured LBD (4). LLM is not electrophilic and hence a covalent interaction is not expected. However, molecular docking identified a binding-pocket for LLM in AR (Fig. 4A). The bottom of the LLM-binding pocket is formed by the side chains of A735, Y739, P817, and V821. The hydroxyl group of Y739 is positioned to form an on-face hydrogen bond with the π-electron cloud of the LLM phenyl ring system. The wall of the pocket is formed by the K822, K731, M734, K905, and Q902 side chains, among which the K905 and Q902 are in close contact with LLM. One side of the LLM-binding pocket is open. On the left-hand side of the opening as shown in Fig. 4A is located the D819 side chain. Potentially, the D819 side chain carboxyl group is able to form a salt bridge with the LLM amine group. A salt bridge is the combination of hydrogen bonding and electrostatic interactions. It may contribute significantly to the stability of the LLM:AR-LBD complex.

We tested the functional significance of one of these potential interactions using PC-3 cell line, which lacks AR expression. As can be seen in Fig. 4B, overexpression of the wild-type (WT) AR in PC-3 cells resulted in an increase in probasin luciferase activity in the presence of R1881, which was decreased significantly by LLM treatment. The Y739A mutation significantly attenuated LLM-mediated suppression of probasin luciferase reporter activity (Fig. 4B). The LLM-mediated suppression of AR protein was also abolished by Y739A mutation. LLM treatment decreased AR protein level in PC-3 cells overexpressing WT AR (Fig. 4C).

The role of amine group in AR inhibition by LLM

We used an analog of LLM, dehydroabietyl isothiocyanate (LLM-ITC; structure is shown in Fig. 5A), to further understand the significance of amine group in AR suppression by LLM. Molecular docking revealed a different mode of interaction between LLM-ITC and AR LBD (Fig. 5B). The protein levels of full-length AR, splice variants of AR, or PSA were not decreased by LLM-ITC treatment in 22Rv1, LNCaP, or AR overexpressing PC-3 cells (Fig. 5C; Supplementary Fig. S7). In addition, both 22Rv1 and LNCaP cells were significantly more resistant to growth inhibition by LLM-ITC treatment (Fig. 5D) in comparison with LLM (Fig. 1B). Consistent with these results, probasin luciferase activity was not affected by LLM-ITC treatment (Fig. 5E). Collectively, these results indicated a critical role for the amine group in suppression of cell growth and AR by LLM.

In vivo downregulation of AR, AR-V7, and PSA in 22Rv1 xenografts

We used the 22Rv1 xenograft model for the *in vivo* studies because: (a) this cell line rapidly develops tumor upon implantation as compared to LNCaP cells, and (b) unlike LNCaP, the 22Rv1 cell line allows determination of the effect of LLM treatment on protein levels of both full-length AR and its splice variants. Figure 6A shows tumor volume in individual mouse of the control and the LLM treatment group. The mean tumor volume was lower by 34% in the LLM treatment group compared with control but the difference was insignificant due to large data scatter and a small sample size. Figure 6B depicts representative immunohistochemistry for Ki-67 and H&E staining for tumor of a control mouse and a

tumor of LLM-treated mouse. The Ki-67 expression as well as mitotic count was significantly lower in the tumors of LLM-treated mice compared with control (Fig. 6C). Figure 6D shown western blots for AR, AR-V7 and PSA using tumor supernatants of control and LLM-treated mice. Expression of both full-length AR and AR-V7 were significantly lower in the tumors of LLM-treated mice in comparison with controls (Fig. 6E). In addition, tumor expression of PSA protein (Fig. 6F) as well as its circulating level (Fig. 6G) was significantly lower in LLM treatment group compared with control. LLM treatment did not cause weight loss or any other side effects (Supplementary Fig. S8). These results indicated downregulation of AR and its target PSA *in vivo* upon LLM administration to 22Rv1 xenograft bearing mice.

Discussion

The present study is the first to show inhibitory effect of LLM on AR in prostate cancer cells. We also found that LLM inhibits growth prostate cancer cells that are resistant to clinically used antiandrogen enzalutamide due to expression of AR-V7. The LLM-mediated inhibition of prostate cancer cell growth is accompanied by downregulation of AR and its target PSA both *in vitro* and *in vivo*. It is important to point out that growth inhibition and AR downregulation by LLM treatment is observed at pharmacological doses.

The present study suggests a critical role for non-covalent interactions of LLM with A735, Y739, P817, V821, K822, K731, M734, K905, and Q902 of AR LBD. The fact that AR downregulation and transcriptional activity inhibition by LLM is abolished by Y739A mutation of AR provides experimental evidence for functional significance of one of the interactions. However, other interactions may also be important. For example, the nuclear/cytoplasmic shuttling of AR is regulated by a nuclear localization signal (residues 617–633) at the junction of DNA-binding domain and the hinge region (29, 30) and a ligand-regulated nuclear export signal (residues 742–817) (31). Because LLM interacts with P817, the possibility that this interaction is responsible for LLM-mediated inhibition of nuclear localization of the AR protein cannot be excluded. However, further studies are needed to explore this possibility. LLM decreases protein level of AR-V7 that lacks LBD domain of AR. It is possible that abrogation of AR activation of the probasin target promoter by overexpression of AR-Y739A is due to increased abundance of the mutant protein and probably its half-life. Further work is also necessary to test this possibility.

On one hand, the present study suggests that non-covalent interaction with residues in AR LBD including P817 may contribute to AR inhibition by LLM as the ITC derivative, which does not interact with this AR LBD domain, loses its efficacy. On the other hand, LLM is effective against AR-V7, which lacks the LBD and hence the amino acids for non-covalent interactions, indicating that the primary mechanism of its action is likely through inhibition of AR promoter activity. LLM may even work against an overlapping transcriptional mechanism as evidenced by its ability to inhibit AR-dependent anchorage-independent growth of PC3-AR cells.

Even though LLM administration to 22Rv1 xenograft bearing SCID mice resulted in statistically significant decreases in expression of AR and PSA, the tumor volume was not

significantly different between the control and LLM treatment groups possibly due to a few outliers. The LLM dose used in the present is about 40% of the maximally-tolerated dose of LLM (21). Thus, it is possible that the higher concentrations of LLM are effective for growth inhibition cannot be ruled out without further experimentation.

The mechanistic understanding of the antitumor effect of LLM is restricted to a few publications using melanoma cell lines (21, 22). Antitumor effect of LLM in melanoma cell lines *in vitro* and *in vivo* was associated with inhibition of Akt, Stat3, and Erk1/2 activation (reduced phosphorylation) (21, 22). The inhibition of these prosurvival and oncogenic pathways upon LLM treatment was observed as early as 3 hours after treatment at 3–5 μmol/L concentrations (21, 22). However, the precise role and contribution of these pathways in growth inhibition and cell death induction by LLM is still unclear. Studies have also shown that ectopic expression of AR in PC-3 renders them more susceptible to apoptosis (32). The present study does reveal proapoptotic effect of LLM. However, it is possible that LLM-induced apoptosis in prostate cancer cells is mediated by modulation of Akt, Stat3 and/or Erk1/2. Further studies are needed to explore the role of Akt, Stat3, and Erk1/2 in possible apoptosis induction by LLM in prostate cancer cells.

Despite exciting mechanistic insights presented in this study, further pre-clinical studies are needed in preparation for the clinical development of LLM, including (a) determination of the dose-response effect of LLM treatment on *in vivo* growth of prostate cancer cells other than 22Rv1 (LNCaP and C4–2B) as well as patient-derived xenografts, (b) determination of the oral bioavailability of LLM and a careful analysis of the clinical pharmacology and metabolism of LLM, (c) determination of an appropriate dosing schedule of LLM that could then be taken in to the clinic, and (e) determination of the toxicity profile of LLM administration by analyzing a wide range of normal host tissues. If LLM is found to be well-tolerated in the mouse model, additional toxicology studies in a larger-sized animal model to determine the safety of this agent will be required. The findings from these pre-clinical studies should then provide the rational basis for designing the first-in-man phase I clinical studies of LLM.

In summary, the results of the present study indicate that AR is a novel mechanistic target of prostate cancer cell growth inhibition by LLM. We also provide *in vitro* (human and murine prostate cancer cell lines) and *in vivo* (22Rv1 xenografts in SCID mice) evidence for inhibition of AR expression and activity following LLM treatment. Finally, the present study reveals that non-covalent interactions of LLM with AR LBD are functionally important.

Supplementary Material

Refer to Web version on PubMed Central for supplementary material.

Acknowledgments

Grant Support

This work was supported by the grant RO1 CA101753 awarded by the National Cancer Institute (S.V. Singh) and the Intramural Research Program of the NIH, National Cancer Institute, Center for Cancer Research (X. Ji). This

research used the Animal Facility and the Tissue and Research Pathology Facility supported in part by Cancer Center Support Grant from the National Cancer Institute (P30 CA047904; Robert L. Ferris- Principal Investigator).

References

1. Siegel RL, Miller KD, Jemal A. Cancer statistics, 2018. CA Cancer J Clin 2018;68:7–30. [PubMed: 29313949]
2. Shand RL, Gelmann EP. Molecular biology of prostate-cancer pathogenesis. Curr Opin Urol 2006;16:123–31. [PubMed: 16679847]
3. Schmidt LJ, Tindall DJ. Androgen receptor: past, present and future. Curr Drug Targets 2013;14:401–7. [PubMed: 23565753]
4. Tan MHE, Li J, Xu HE, Melcher K, Yong EL. Androgen receptor: structure, role in prostate cancer and drug discovery. Acta Pharmacol Sinica 2015;363–23.
5. Sharifi N, Gulley JL, Dahut WL. An update on androgen deprivation therapy for prostate cancer. Endocr Relat Cancer 2010;17:R305–15. [PubMed: 20861285]
6. Lu-Yao GL, Albertsen PC, Moore DF, Shih W, Lin Y, DiPaola RS, et al. Fifteen-year survival outcomes following primary androgen-deprivation therapy for localized prostate cancer. JAMA Intern Med 2014;174:1460–7. [PubMed: 25023796]
7. de Bono JS, Logothetis CJ, Molina A, Fizazi K, North S, Chu L, et al. Abiraterone and increased survival in metastatic prostate cancer. N Engl J Med 2011;364:1995–2005. [PubMed: 21612468]
8. Scher HI, Beer TM, Higano CS, Anand A, Taplin ME, Efstathiou E, et al. Antitumour activity of MDV3100 in castration-resistant prostate cancer: a phase 1–2 study. Lancet 2010;375:1437–46. [PubMed: 20398925]
9. Antonarakis ES, Lu C, Wang H, Luber B, Nakazawa M, Roeser JC, et al. AR-V7 and resistance to enzalutamide and abiraterone in prostate cancer. N Engl J Med 2014;371:1028–38. [PubMed: 25184630]
10. Ryan CJ, Tindall DJ. Androgen receptor rediscovered: the new biology and targeting the androgen receptor therapeutically. J Clin Oncol 2011;29:3651–8. [PubMed: 21859989]
11. Feldman BJ, Feldman D. The development of androgen-independent prostate cancer. Nat Rev Cancer 2001;1:34–45. [PubMed: 11900250]
12. Shafi AA, Yen AE, Weigel NL. Androgen receptors in hormone-dependent and castration-resistant prostate cancer. Pharmacol Ther 2013;140:223–38. [PubMed: 23859952]
13. Watson PA, Arora VK, Sawyers CL. Emerging mechanisms of resistance to androgen receptor inhibitors in prostate cancer. Nat Rev Cancer 2015;15:701–11. [PubMed: 26563462]
14. Visakorpi T, Hyytinen E, Koivisto P, Tanner M, Keinänen R, Palmberg C, et al. In vivo amplification of the androgen receptor gene and progression of human prostate cancer. Nat Genet 1995;9:401–6. [PubMed: 7795646]
15. Gottlieb B, Beitel LK, Nadarajah A, Paliouras M, Trifiro M. The androgen receptor gene mutations database: 2012 update. Hum Mutat 2012;33:887–94. [PubMed: 22334387]
16. Guo Z, Yang X, Sun F, Jiang R, Linn DE, Chen H, et al. A novel androgen receptor splice variant is up-regulated during prostate cancer progression and promotes androgen depletion-resistant growth. Cancer Res 2009;69:2305–13. [PubMed: 19244107]
17. Watson PA, Chen YF, Balbas MD, Wongvipat J, Socci ND, Viale A, et al. Constitutively active androgen receptor splice variants expressed in castration-resistant prostate cancer require full-length androgen receptor. Proc Natl Acad Sci USA 2010;107:16759–65. [PubMed: 20823238]
18. Mellinghoff IK, Vivanco I, Kwon A, Tran C, Wongvipat J, Sawyers CL. HER2/neu kinase-dependent modulation of androgen receptor function through effects on DNA binding and stability. Cancer Cell 2004;6:517–27. [PubMed: 15542435]
19. Kaur M, Agarwal R. Transcription factors: molecular targets for prostate cancer intervention by phytochemicals. Curr Cancer Drug Targets 2007;7:355–67. [PubMed: 17979630]
20. Li X, Liu Z, Xu X, Blair CA, Sun Z, Xie J, et al. Kava components down-regulate expression of AR and AR splice variants and reduce growth in patient-derived prostate cancer xenografts in mice. PLoS One 2012;7:e31213. [PubMed: 22347450]

21. Gowda R, Madhunapantula SV, Kuzu OF, Sharma A, Robertson GP. Targeting multiple key signaling pathways in melanoma using leelamine. Mol Cancer Ther 2014;13:1679–89. [PubMed: 24688050]

22. Kuzu OF, Gowda R, Sharma A, Robertson GP. Leelamine mediates cancer cell death through inhibition of intracellular cholesterol transport. Mol Cancer Ther 2014;13:1690–703. [PubMed: 24688051]

23. Xiao D, Choi S, Johnson DE, Vogel VG, Johnson CS, Trump DL, et al. Diallyl trisulfide-induced apoptosis in human prostate cancer cells involves c-Jun N-terminal kinase and extracellular-signal regulated kinase-mediated phosphorylation of Bcl-2. Oncogene 2004;23:5594–606. [PubMed: 15184882]

24. Xiao D, Srivastava SK, Lew KL, Zeng Y, Hershberger P, Johnson CS, Trump DL, Singh SV. Allyl isothiocyanate, a constituent of cruciferous vegetables, inhibits proliferation of human prostate cancer cells by causing G_2/M arrest and inducing apoptosis. Carcinogenesis 2003;24:891–7. [PubMed: 12771033]

25. Hahm ER, Karlsson AI, Bonner MY, Arbiser JL, Singh SV. Honokiol inhibits androgen receptor activity in prostate cancer cells. Prostate 2014;74:408–20. [PubMed: 24338950]

26. Powolny AA, Bommareddy A, Hahm ER, Normolle DP, Beumer JH, Nelson JB, et al. Chemopreventative potential of the cruciferous vegetable constituent phenethyl isothiocyanate in a mouse model of prostate cancer. J Natl Cancer Inst 2011;103:571–84. [PubMed: 21330634]

27. Hahm ER, Lee J, Kim SH, Sehrawat A, Arlotti JA, Shiva SS, et al. Metabolic alterations in mammary cancer prevention by withaferin A in a clinically relevant mouse model. J Natl Cancer Inst 2013;105:1111–22. [PubMed: 23821767]

28. Song M, Lee D, Lee T, Lee S. Determination of leelamine in mouse plasma by LC-MS/MS and its pharmacokinetics. J Chromatogr B Analyt Technol Biomed Life Sci 2013;931:170–3.

29. Zhou ZX, Sar M, Simental JA, Lane MV, Wilson EM. A ligand-dependent bipartite nuclear targeting signal in the human androgen receptor. Requirement for the DNA-binding domain and modulation by NH2-terminal and carboxyl-terminal sequences. J Biol Chem 1994;269:13115–23. [PubMed: 8175737]

30. Jenster G, Trapman J, Brinkmann AO. Nuclear import of the human androgen receptor. Biochem J 1993;293:761–8. [PubMed: 8352744]

31. Saporita AJ, Zhang Q, Navai N, Dincer Z, Hahn J, Cai X, et al. Identification and characterization of a ligand-regulated nuclear export signal in androgen receptor. J Biol Chem 2003;278:41998–42005. [PubMed: 12923188]

32. Heisler LE, Evangelou A, Lew AM, Trachtenberg J, Elsholtz HP, Brown TJ. Androgen-dependent cell cycle arrest and apoptotic death in PC-3 prostatic cell cultures expressing a full-length human androgen receptor. Mol Cell Endocrinol 1997;126:59–73. [PubMed: 9027364]

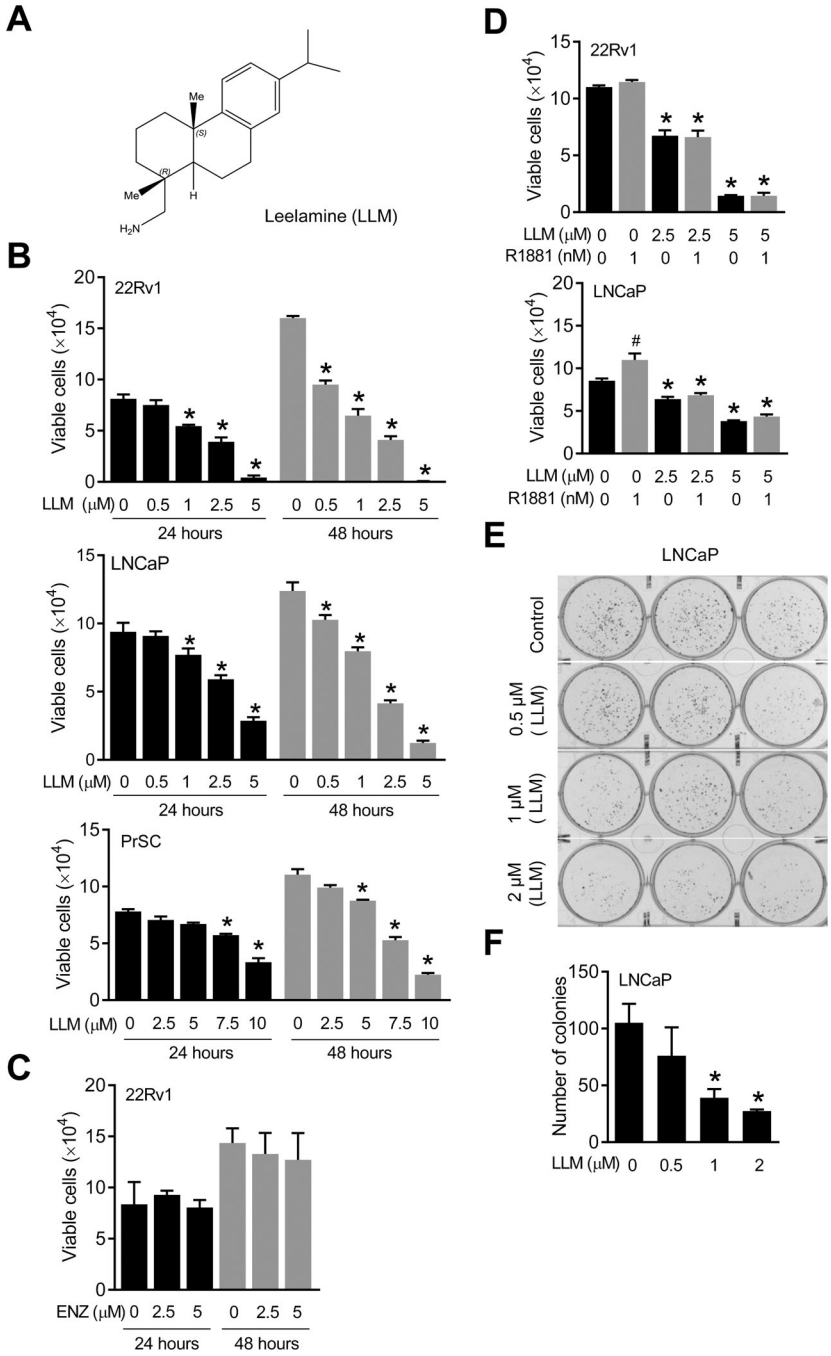

Figure 1.

LLM treatment inhibited viability of prostate cancer cells. **(A)** Chemical structure of LLM. **(B)** Effect of LLM treatment on viability of 22Rv1, LNCaP, or PrSC cells as determined by trypan blue dye exclusion assay. **(C)** Effect of enzalutamide treatment on viability of 22Rv1 cells as determined by trypan blue dye exclusion assay. For data in panels **B** and **C**, combined results from two different experiments are shown as mean ± SD (n = 6). *Significantly different ($p<0.05$) compared with ethanol-treated control by one-way ANOVA followed by Dunnett's test. **(D)** Effect of LLM treatment on viability of 22Rv1 and

LNCaP cells with or without treatment with a synthetic androgen (R1881). Combined results from two different experiments are shown as mean ± SD (n = 6). Significantly different ($p<0.05$) *compared with ethanol-treated control and #between with or without R1881 treatment by one-way ANOVA followed by Bonferroni's test. Clonogenic assay **(E)** and quantitation **(F)** in LNCaP cells after 10 days of treatment with LLM or ethanol (control). Results shown are mean ± SD (n= 3). *Significant ($p<0.05$) compared with control by one-way ANOVA followed by Dunnett's test.

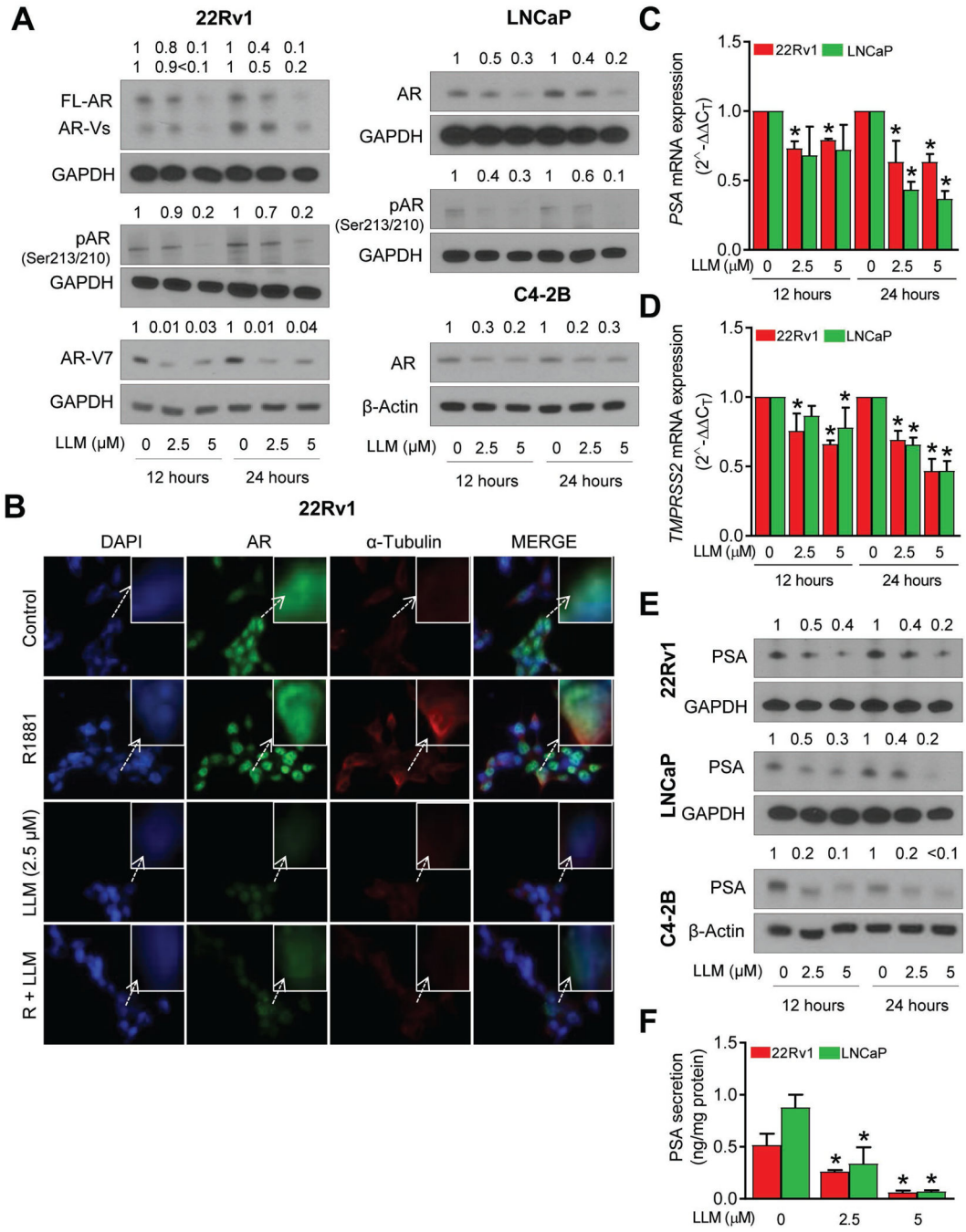

Figure 2.

LLM treatment downregulated AR expression in prostate cancer cells. **(A)** Immunoblotting for full-length AR, splice variants of AR (AR-Vs), phospho-AR (Ser213/210), AR-V7, and GAPDH using lysates from 22Rv1, LNCaP or C4–2B cells after 12 hours or 24 hours of treatment with ethanol and LLM. Numbers above bands represent quantitation of protein expression changes relative to corresponding ethanol control after normalization for GAPDH or β-actin. **(B)** Immunocytochemistry for AR in 22Rv1 cells. Cells were pre-treated with specified concentration of LLM for 3 hours followed by incubation with 1 nmol/L

R1881 for additional 9 hours. Each experiment was repeated at least two times with comparable results. RT-PCR data showing effect of LLM treatment (12 hours) on mRNA levels of *PSA* **(C)** and *TMPRSS2* in 22Rv1 and LNCaP cells **(D)**. Results shown are mean ± SD (n= 6). *Significantly different ($p<0.05$) compared with corresponding ethanol treated control by one-way ANOVA followed by Dunnett's test. **(E)** Immunoblotting for PSA using lysates from 22Rv1, LNCaP, or C4–2B cells after treatment with ethanol or the indicated concentrations of LLM. The numbers on top of the bands indicate changes in PSA protein level compared to the corresponding ethanol-treated control. **(F)** Effect of LLM treatment on PSA secretion in conditioned media following a 24-hour treatment of 22Rv1 and LNCaP cells with ethanol or LLM. Results shown are mean ± SD (n= 6). *Significantly different ($p<0.05$) compared with corresponding ethanol-treated control by one-way ANOVA followed by Dunnett's test. Comparable results were observed in replicate experiments.

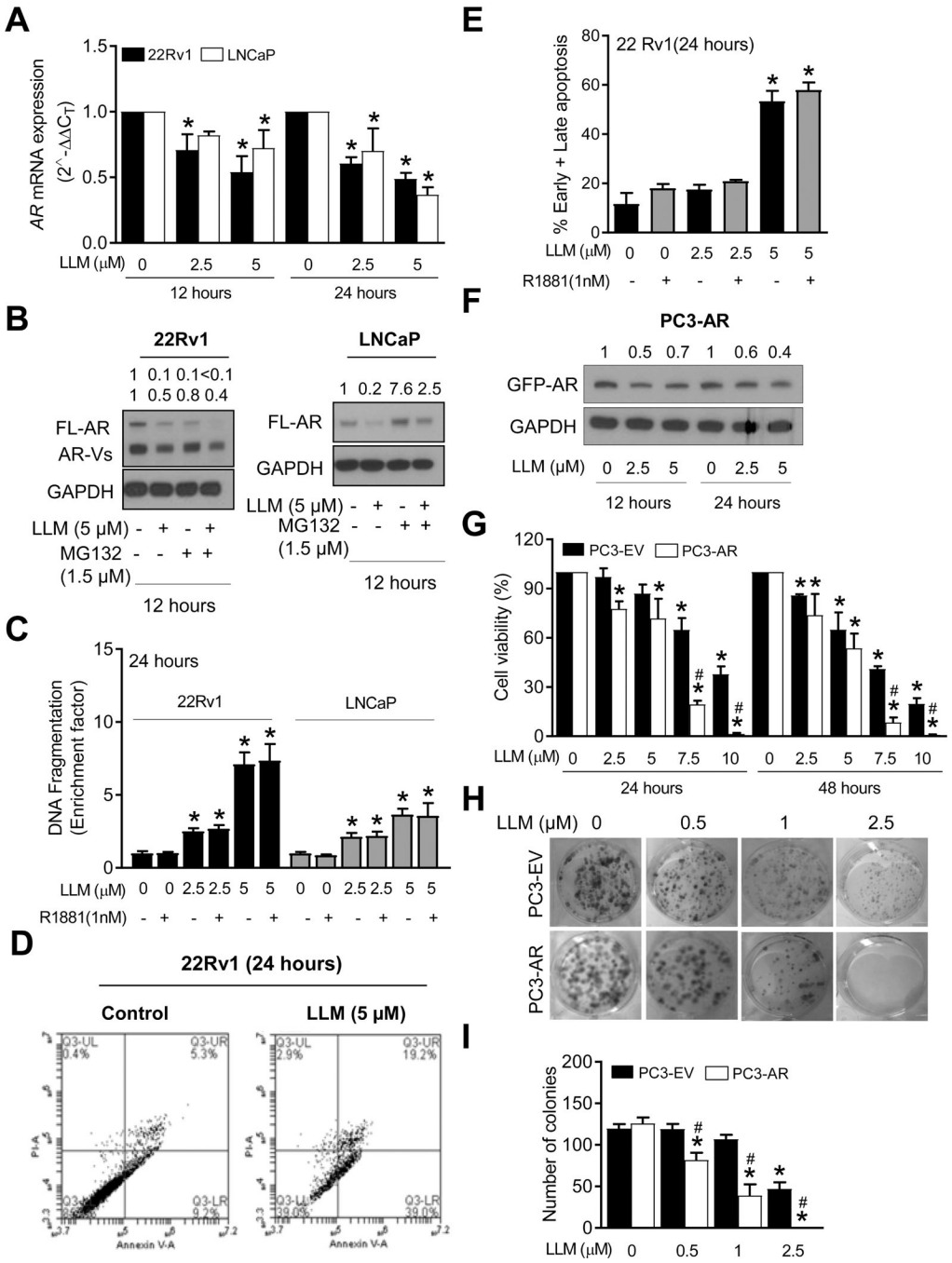

Figure 3.

LLM treatment downregulated *AR* expression in prostate cancer cells. **(A)** mRNA expression level of *AR* in 22Rv1 and LNCaP cells after treatment with ethanol or the indicated concentrations of LLM. Results shown are mean ± SD (n= 6). * Significantly different ($p<0.05$) compared with ethanol-treated control by one-way ANOVA followed by Dunnett's test. **(B)** Western blotting for full-length AR and AR-Vs using lysates from 22Rv1 and LNCaP cells after treatment with MG132 (1 hour of pre-treatment) and/or LLM (12 hours of treatment). **(C)** Quantitation of histone-associated DNA fragment release into the

cytosol in 22Rv1 and LNCaP cells after 24-hour treatment with indicated doses of LLM in the absence or presence of 1 nmol/L R1881. (**D)** Representative flow histograms depicting early (Annexin V-high, propidium iodidelow) and late apoptotic fraction (Annexin V-high, propidium iodide-high) in 22Rv1 cells after 24-hour treatment with ethanol or LLM in the absence or presence of 1 nmol/L R1881. **(E)** Quantitation of apoptotic fraction in 22Rv1 cells after 24-hour treatment with indicated doses of LLM alone or in combination with 1 nmol/L R1881. Experiment was repeated twice in triplicate and representative data from one such experiment is shown as mean ± SD (n=3). *Significantly different ($p<0.05$) compared with control by one-way ANOVA followed by Bonferroni's test. **(F)** Western blotting for GFP-AR using lysates from PC3-AR cells after treatment with ethanol or the indicated concentrations of LLM. **(G)** Effect of LLM treatment on viability of PC-3 cells stably transfected with empty pCMV vector (PC3-EV) or the same vector encoding GFP-AR (PC3-AR). Significantly different ($p<0.05$) *compared with corresponding ethanol-treated control, and #between PC3-EV vs PC3-AR by one-way ANOVA followed by Bonferroni's multiple comparisons test. Clonogenic assay **(H)** and quantitation of clonogenic data **(I)** for PC3-EV and PC3-AR cells after treatment with ethanol or the indicated concentrations of LLM. Results shown are mean ± SD (n=3). Significantly different ($p<0.05$) *compared with corresponding ethanol-treated control, and #between PC3-EV and PC3-AR cells by one-way ANOVA followed by Bonferroni's multiple comparisons test. Comparable results were observed in replicate experiments.

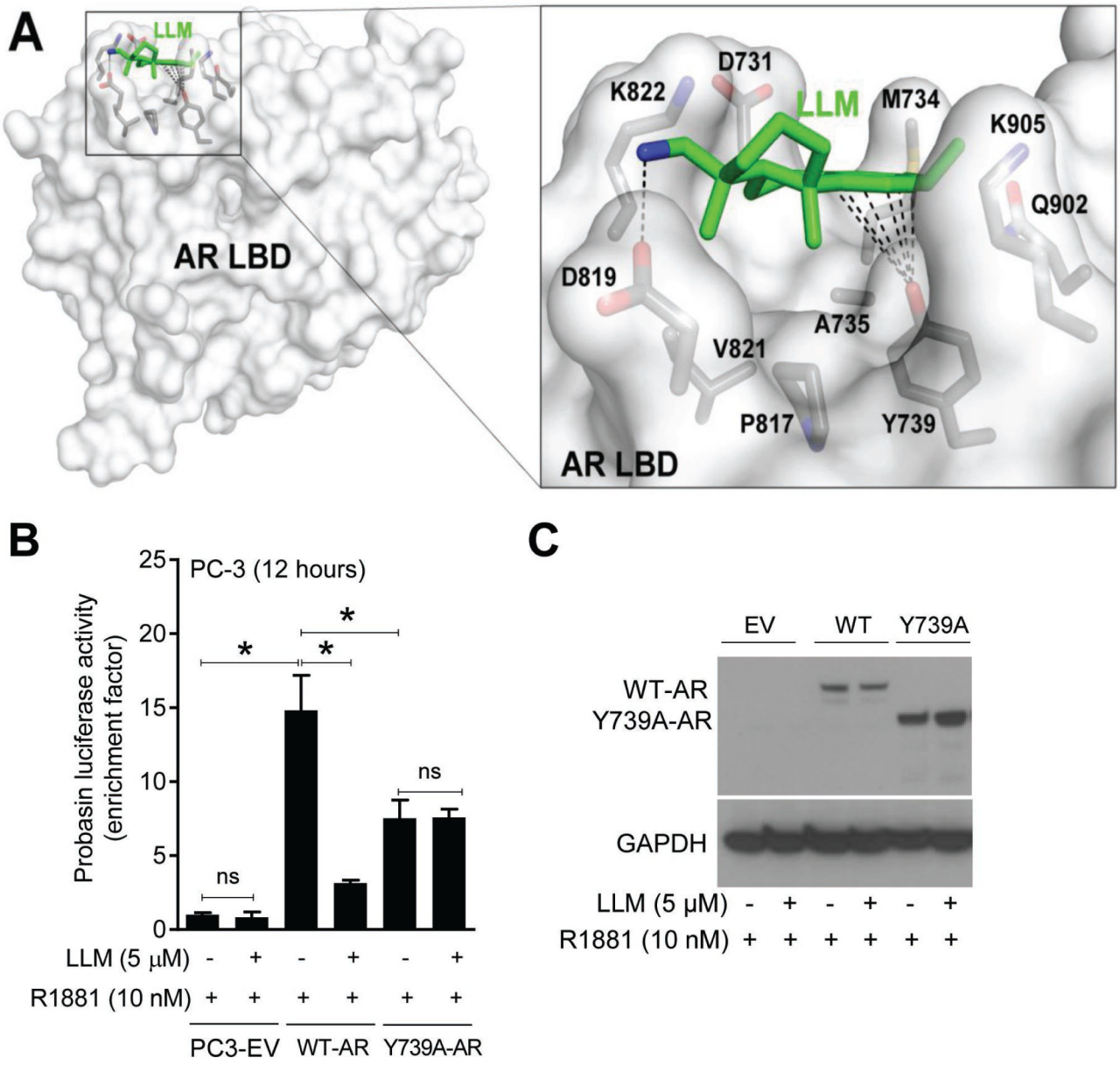

Figure 4.

LLM interacted with amino acid residues in AR LBD. **(A)** Docking of the LLM molecule in human AR LBD. Overall view of the docking model of the LLM:AR-LBD complex (left panel). The human AR LBD is shown as a transparent molecular surface in white. The LLM molecule is shown as a stick model (C in green, N in blue). The amino acid side chains in contact with LLM are shown as stick models in the right panel (C in grey, N in blue, O in red, P in orange). **(B)** Effect of LLM treatment (12 hours) on probasin luciferase reporter activity in PC-3 cells transiently transfected with empty vector (PC3-EV), wild-type AR (WT-AR), or Y739A mutant of AR (Y739A-AR) with or without treatment with R1881. Results shown are mean ± SD (n=6). *Significantly different ($p<0.05$) between the indicated groups by one-way ANOVA followed by Bonferroni's multiple comparisons test (ns = not significant). **(C)** Western blotting for AR protein using lysates from PC3 cells transfected

with EV, WT-AR, and Y739A mutant of AR. Cells were treated with ethanol or LLM in the presence of 10 nmol/L R1881 for 12 hours. Comparable results were observed in replicate experiments.

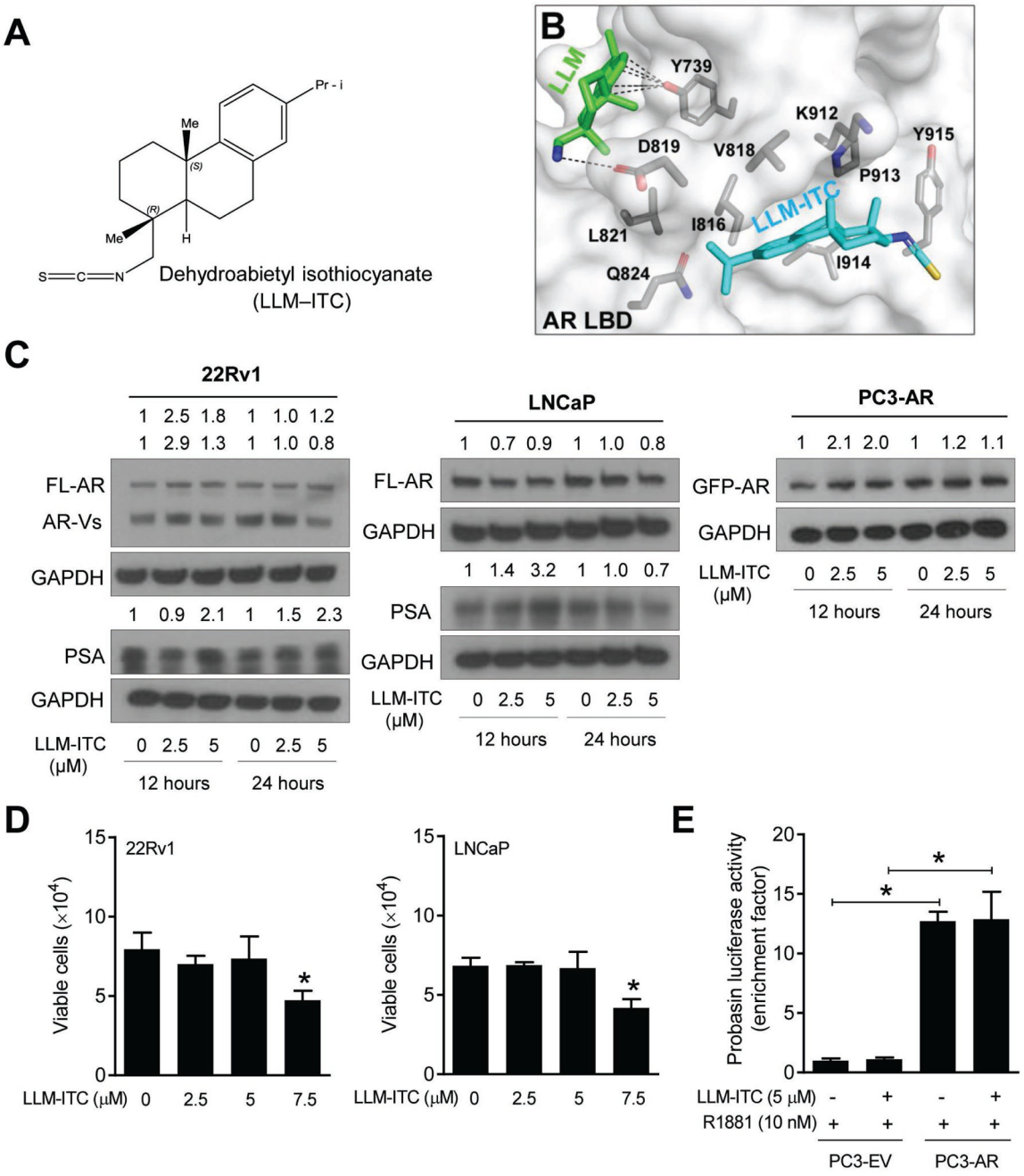

Figure 5.

Effect of dehydroabietyl isothiocyanate (LLM-ITC) on AR expression in prostate cancer cells. **(A)** Chemical structure of LLM-ITC. **(B)** Docking of the LLM-ITC molecule in human AR LBD. The human AR LBD is shown as a transparent molecular surface in white. The LLM-ITC molecule is shown as a stick model (C in cyan, N in blue, and S in orange). The amino acid side chains in contact with LLM-ITC are shown as stick models (C in grey, N in blue, and O in red). For comparison, the LLM-binding site is indicated with the LLM molecule (C in green) in the LLM:AR-LBD model illustrated in Figure 4A, highlighting that

LLM-ITC recognizes a distinct pocket on the surface of AR LBD and that the interaction between LLM-ITC and ARLBD is purely hydrophobic in nature. **(C)** Immunoblotting for full-length AR (FL-AR), AR-Vs, PSA, and GAPDH using lysates from 22Rv1, LNCaP, and PC3-AR cells treated with solvent control or LLM. The numbers on top of the bands indicate changes in protein levels compared to the corresponding solvent control. **(D)** Effect of LLM-ITC on viability of 22Rv1 and LNCaP cells after 24 hours of treatments as determined by trypan blue dye exclusion assay. Combined results from two independent experiments are shown as mean ± SD (n = 6). *Significantly different ($P<0.05$) compared with control by one-way ANOVA followed by Dunnett's test. **(E)** Probasin luciferase activity in PC3-EV and PC3-AR cells after treatment with solvent control or LLM-ITC in presence of 10 nmol/L R1881 (12 hours of treatment). Results shown are mean ± SD (n=3). *Significantly different ($P<0.05$) between the indicated groups by one-way ANOVA followed by Bonferroni's test. Similar results were observed in replicate experiments.

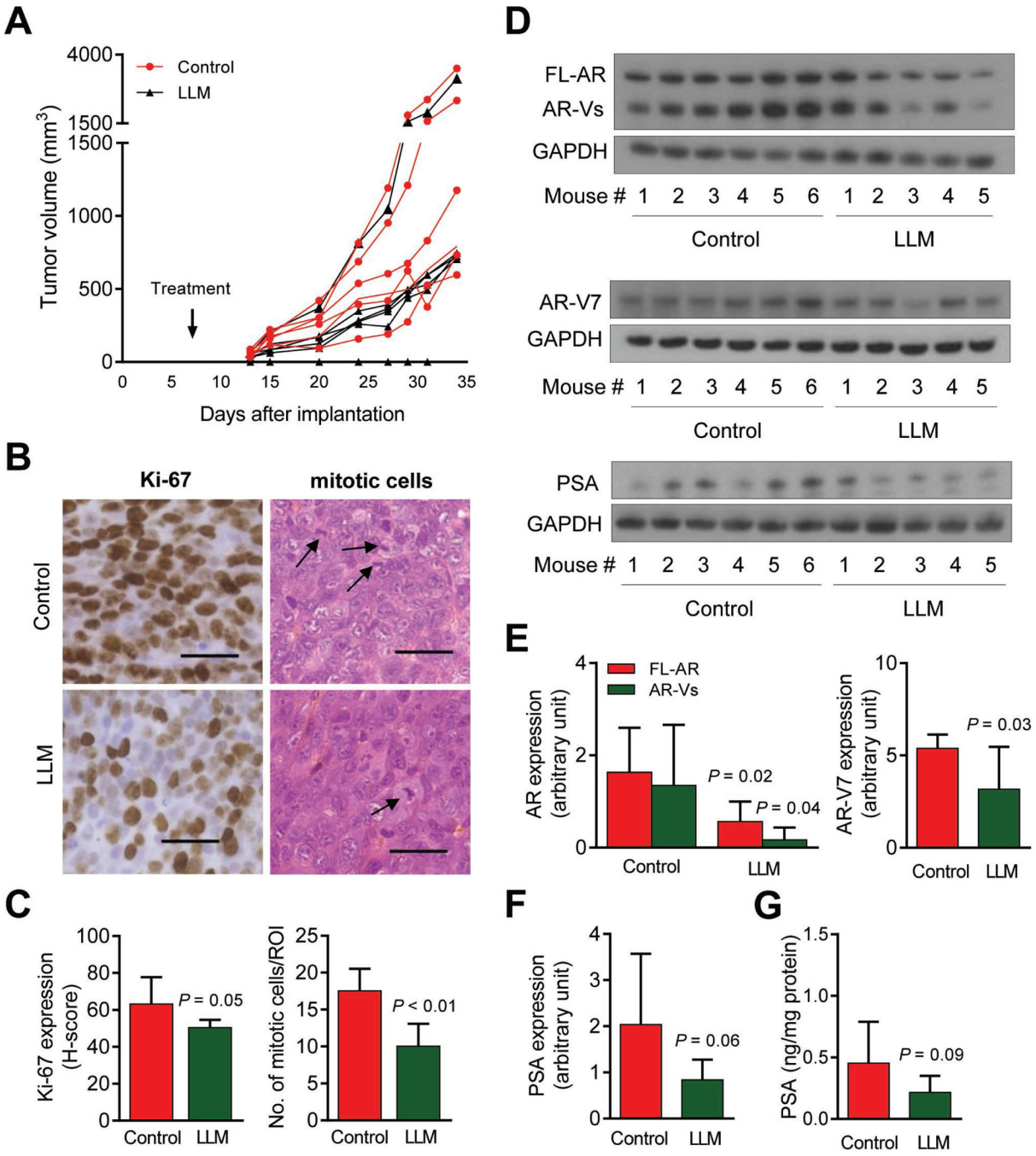

Figure 6.

LLM administration downregulated expression of AR, AR-V7, and PSA in 22Rv1 xenografts *in vivo*. **(A)** Tumor volume over time in mice administered with either vehicle or 9.1 mg/kg LLM. Results shown are mean ± SD (n = 5–6). **(B)** Immunohistochemistry for Ki-67 expression and H&E staining for mitotic bodies in a representative mouse of the LLM treatment group and a mouse of the control group (×400 magnification, scale bar = 100 μm). **(C)** Quantitation of Ki-67 expression (H-score) and number of mitotic cells/region of interest (ROI). Results shown are mean ± SD (n = 5–6). Statistical significance was

determined by Student's t-test. **(D)** Western blotting for AR, AR-V7, and PSA proteins using supernatants from 22Rv1 tumor xenografts from control and LLM-treated mice. **(E)** Densitometric quantitation of AR and AR-V7 expression in 22Rv1 tumors. The results shown are mean ± SD (n = 5–6). Statistical significance was determined by Student's t-test. **(F)** Densitometric quantitation of PSA expression in 22Rv1 tumors. The results shown are mean ± SD (n = 5–6). Statistical significance was determined by Student's t-test. **(G)** Circulating levels of PSA in the plasma of control and LLM-treated mice. The results shown are mean ± SD (n = 5–6). Statistical significance was determined by Student's t-test.